DOI: 10.1021/ma902136a

Macromolecules
ARTICLE

Temperature-Induced Control of Conformation and Conjugation Length in Water-Soluble Fluorescent Polythiophenes

Jinwoo Choi,[†] Carmen R. Ruiz,[‡] and Evgueni E. Nesterov*[,†]

[†]*Department of Chemistry and* [‡]*Department of Biological Sciences, Louisiana State University, Baton Rouge, Louisiana 70803*

Received September 25, 2009; Revised Manuscript Received December 18, 2009

ABSTRACT: Application of fluorescent polythiophenes and related conjugated polymers as a platform for highly sensitive chemo- and biodetection can benefit from the possibility to effectively control their conformation and conjugation length by applying external stimuli. Temperature can be used as such a stimulus if a substantial effect can be achieved in a relatively narrow temperature range. To investigate the temperature-induced conformational switching, a series of polythiophenes with different degree of regioregularity were prepared and functionalized by grafting temperature-responsive poly(*N*-isopropylacrylamide) (PNIPAm) side chains to their conjugated backbones. These highly water-soluble fluorescent brush-type copolymers featured almost complete lack of intermolecular electronic interactions even in aggregated state owing to remarkably insulating properties of the PNIPAm grafts. Therefore, these grafted copolymers provided an opportunity to study the effects originating from the conformational switching within isolated individual polymer chain, without any impact from interchain interactions. The unique property of PNIPAm—hydrophilic extended coil to hydrophobic collapsed globule phase transition occurring in a very narrow temperature interval—resulted in reversible temperature-induced twisting of the polythiophene conjugated backbone, which was accompanied by pronounced spectroscopic changes. Remarkably, both the extent and appearance of the conformational twisting were found to be strongly dependent on regioregularity of the polythiophene backbone. Low regioregularity copolymer showed much smaller magnitude of the conformational twisting yielding only subtle spectral changes which occurred as a threshold process in a narrow temperature interval. In contrast, higher regioregularity copolymers demonstrated large conformational twisting and substantial spectral changes occurring continuously in a broad temperature interval. A qualitative explanation of this phenomenon was proposed based on the results of spectroscopic, thermal, and light-scattering experiments.

Introduction

The universal application of conjugated polymers (CPs) as signal-generating media in chemo- and biosensors is based on the efficient transport of excited states (excitons) along the polymer chain. The exciton migration allows delivery of photoexcitation energy absorbed over large areas into low-energy gap sites created by the binding of analytes or other minor perturbations, resulting in significant signal amplification in sensory devices.[1,2] The process of intramolecular energy migration is strongly dependent on the extent of π-electron conjugation along the CP chain, which is determined by the ability of the polymer to achieve a highly planarized conjugated backbone conformation.[3] Furthermore, the CP backbone conformation can change as a result of intermolecular aggregation or interaction of an individual polymer chain with bioanalytical targets which can lead to a pronounced spectroscopic response, the phenomenon which provides a universal foundation for the development of biosensors and fluorescent biomarkers. For such applications, water-soluble CPs are especially promising and were the subject of extensive studies in recent years.[4] Among various classes of CPs, water-soluble polythiophenes (PTs) possessing solubilizing ionic or noncharged hydrophilic side chains are particularly interesting as they are highly susceptible to induced conformational changes of the conjugated backbone, which result in the wavelength shifts and intensity attenuations in absorption and fluorescence spectra and provide a simple basis for numerous bioanalytical applications.[5] Because of the intrinsic hydrophobicity of the polythiophene conjugated backbone, even polymers substituted with hydrophilic solubilizing side groups tend to form intermolecular aggregates in dilute aqueous solutions as a way to minimize unfavorable contacts with solvent molecules. More planarized conformations of PTs tend to exhibit even stronger hydrophobic interchain interactions leading to significant intermolecular aggregation, whereas more twisted, lower conjugation length conformations show a smaller extent of aggregation. Such planarization-induced aggregation results in interchain electronic delocalization leading to bathochromic shifts in absorption and emission spectra as well as diminished quantum efficiency of the polymer's fluorescence. These spectroscopic features are exactly the same as those caused by increasing conjugation length upon planarization of an isolated, nonaggregated polymer molecule. As the spectroscopic outcomes of both phenomena parallel each other, it is generally impossible to deconvolute the effect of extending π-electron conjugation length within isolated CP molecule upon its planarization from the effect of the planarization-induced intermolecular aggregation. This resulted in often controversial and contradictory interpretation of molecular mechanisms responsible for spectroscopic changes in water-soluble PTs.[6] From the fundamental standpoint, experimental differentiation between these two phenomena would be important as it could shed some light on the role of through-bond Dexter-type mechanism of intramolecular photoexcitation energy migration, which in extended conjugated systems is often considered

*Corresponding author. E-mail: een@lsu.edu.

 Published on Web 01/25/2010

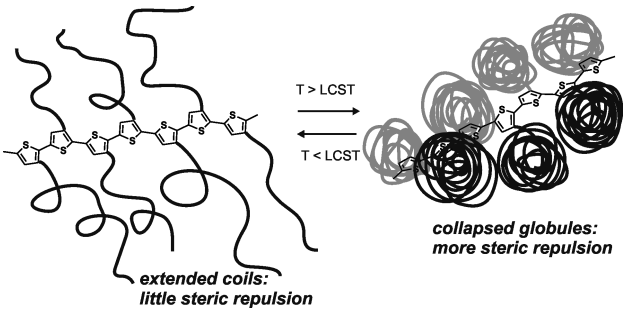

Figure 1. Schematic illustration of the temperature-induced control of PT backbone conformation: grafted PNIPAm side chains collapse into sterically bulkier hydrophobic globular phase at temperatures above LCST, causing torsional twisting of the PT backbone (elements are not to scale).

inefficient and inferior to its through-space Förster-type counterpart.[7] Indeed, the through-bond intramolecular energy migration is expected to depend strongly on the extent of planarity of the conjugated polymer backbone and significantly diminish upon the backbone twisting, while the dipole−induced dipole exciton hopping would be much less affected by the conformational twisting of the individual chain but will be dramatically enhanced due to the possibility of intermolecular energy migration in the three-dimensional polymer aggregates. Therefore, substantial variations of the intramolecular exciton migration efficiency upon induced conformational change in the conjugated backbone of the *isolated* PT chain would indicate an appreciable role of the through-bond mechanism.[3d] From the practical standpoint, the ability to effectively control backbone conformation of the isolated conjugated PT chains in solution would add an extra variable in controlling the sensor behavior of the PT-based chemo- and biodetecting systems.

In the search for possible model PT systems with electronic properties unaffected by aggregation in dilute solutions, and where the conjugated backbone conformation can be controlled by applying an external stimulus, we came across poly(*N*-isopropylacrylamide) (PNIPAm) grafted polythiophenes. PNIPAm is a unique temperature-responsive polymer which, due to its lower critical solution temperature (LCST) appearing in the physiological range (around 32 °C), became very popular as a basis for the development of drug delivery and controlled release scaffolds as well as other biomedical applications.[8] Below LCST, PNIPAm exists in the form of extended, hydrogen bond stabilized random coils, while above LCST it loses water and collapses into tight, hydrophobic globules.[9] The phase transition from coils to collapsed globules caused by increasing temperature occurs in the very narrow interval around LCST and, if polymer concentration in aqueous solution is sufficiently high, results in its aggregation and precipitation. Thus, grafting PNIPAm side chains at the β-position of each thienyl repeating unit in PT would provide a means for an effective control of the conjugated backbone conformation by using temperature as an external stimulus. The schematic illustration of this approach is shown in Figure 1. At lower temperature, the extended hydrated PNIPAm coils behave, within the proximity of the PT conjugated backbone, as smaller size substituents, which do not encounter significant steric repulsive interactions, and therefore allow the conjugated backbone to exist in a more planarized conformation with higher conjugation length. In addition, water-mediated hydrogen bonding between adjacent extended PNIPAm coils can further stabilize the planarized PT conformation. Above LCST, collapse of the side chains into hydrophobic globules effectively converts them to sterically bulky substituents; in order to accommodate these large-size substituents, the conjugated PT backbone must twist and bend into a conformation with lower

Scheme 1. Synthesis of PNIPAm-Grafted Polythiophenes P3a−c[a]

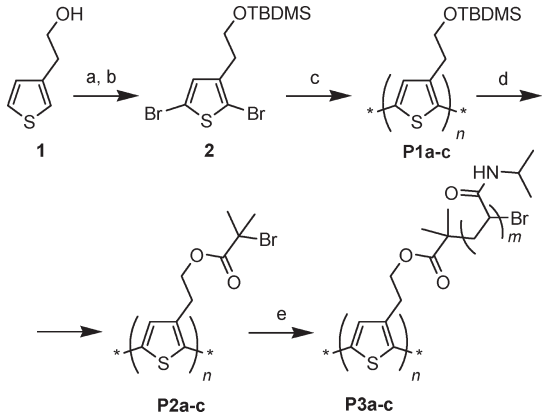

[a] Reagents and conditions: (a) NBS, THF, 0 °C; (b) TBDMS-Cl, imidazole, DMF, 25 °C, 80% over two steps; (c) *tert*-BuMgCl, THF, reflux, followed by $Ni(PPh_3)_2Cl_2$ cat. (for **P1a**), or $Ni(dppp)Cl_2$ cat. (for **P1b−c**), reflux, 20−30%; (d) 2-bromoisobutyryl bromide, TBAF, NEt_3, THF, 25 °C, ∼90%; (e) *N*-isopropylacrylamide, CuBr, 1,4,8,11-tetramethyl-1,4,8,11-tetraazacyclotetradecane, THF, 0 °C, ∼60−70%.

conjugation length (Figure 1). Since the PNIPAm phase transition is reversible, decreasing temperature below LCST would restore the original planarized conformation. In the practical sense, this system would behave as a molecular thermometer, where spectroscopic change (absorption or fluorescence) can be used to report temperature of the surrounding medium.[10] Highly important is that the polymeric PNIPAm grafts would provide an efficient insulation of the individual PT chains. Such insulation can prevent intermolecular electronic interactions between individual PT chains, therefore eliminating aggregation as a factor responsible for spectral properties change and leaving backbone conformation of the isolated PT molecules as the only contributing factor. Recently, McCarley et al. have described a PNIPAm-grafted *regiorandom* PT prepared by chemical oxidative polymerization; in that study, they observed some degree of temperature-induced conformational switching.[11] While the regiorandom nature of their material obviously precluded any significant conformational switching, it also raised a question of the role of regioregularity of the conjugated PT backbone in effecting the conformational control. In this paper, we describe preparation and detailed studies of both regiorandom and regioregular PNIPAm-grafted fluorescent PTs and unexpectedly dramatic effect of small variations in regioregularity on the temperature-induced conformational switching. Such fine control over isolated polymer chain conformation in dilute solutions has not been demonstrated previously and serves to illustrate the relative importance of conformational effects for intramolecular energy migration in conjugated polymers.

Results and Discussion

Synthesis of PNIPAM-Grafted Copolymers. Three conjugated PT precursors **P1a−c** were prepared starting from easily available TBDMS-protected 2,5-dibromothienylethanol **2** (Scheme 1) using nickel-catalyzed McCullough GRIM polymerization method.[12] When $Ni(dppp)Cl_2$ catalyst was used, regioregular polymers were obtained; a series of independent runs afforded the polymers with similar molecular weight and polydispersity values (as determined by GPC analysis) and regioregularities ranging from 89% to 92%. The percent regioregularity in poly(3-alkylthiophene)s refers to the fraction of head-to-tail (HT) coupled repeating units; thus, a 100% regioregular PT has 100% of HT coupling, whereas a polymer with low percentage of HT coupling (50−80%) would be considered regiorandom.[12c,d] Two of

the prepared polymers with HT fraction of 89% and 92% were selected for further studies and designated here as **P1b** and **P1c**, respectively. The percent regioregularity was determined by careful integration of the two signals between 2.5 and 3.5 ppm in ^{1}H NMR spectra; these signals belong to methylene protons of the 3-alkyl chain connected to the thienyl unit and ratio of their integral intensities serves as a reliable measure of regioregularity of 3-alkyl-substituted PTs.[13,14] In order to obtain regiorandom polymer **P1a**, McCullough GRIM polymerization was carried out in the same conditions, but using $Ni(PPh_3)_2Cl_2$ instead of Ni(dppp)Cl_2 as a catalyst. This afforded a polymer with 65% fraction of HT coupled repeating units. The fact that a simple change from bidentate (dppp) to monodentate (PPh_3) ligand in the nickel catalyst led to almost complete loss of regioregularity in the resulting PT has been documented previously;[13b] the likely reason for this phenomenon seems to originate from the less strict steric requirements imposed by the monodentate ligand at the reactive metal center in the rate-limiting oxidative addition step during chain-growth polymerization.[15] Molecular weight of the regioregular polymers **P1b** and **P1c** was found to be higher than that of the random polymer **P1a** (corresponding to ~40 repeating units in **P1b** and **P1c** vs 30 repeating units for **P1a**); this reflected a more "living" nature of the polymerization involving the catalyst with a bidentate ligand.[16]

In the next step, the TBDMS-protected PTs were converted to macroinitiators **P2a**−**c** (Scheme 1). Finding appropriate experimental conditions for carrying out this transformation was a key issue, since both TBDMS protecting groups in **P1a**−**c** and 2-bromoisobutyryl groups in **P2a**−**c** serve as efficient solubilizing substituents for the polymers. However, conversion of **P1a**−**c** to the product polymers **P2a**−**c** occurs through the intermediate formation of OH-terminated side groups which are poor solubilizers for the polymers; polymer with a fraction of these groups exceeding some solubility threshold would become completely insoluble and simply precipitate from solution. In order to avoid precipitation during this transformation, a special strategy was developed to prevent substantial accumulation of OH-terminated side groups during the reaction. In particular, a dilute solution of tetrabutylammonium fluoride (TBAF) was very slowly added using a syringe pump to a THF solution of one of the polymers **P1a**−**c** mixed with an excess of triethylamine and 2-bromoisobutyryl bromide.[17] Employing these conditions allowed avoiding polymer precipitation during the reaction and afforded soluble macroiniators **2a**−**c** in almost quantitative yield. The completeness of side-group transformation was monitored by ^{1}H NMR and was close to 100% in all the runs.

Finally, PNIPAm-grafted polythiophenes **P3a**−**c** were prepared using a well-developed ATRP protocol.[18] Formation of PNIPAm grafts was confirmed by ^{1}H NMR and by significant increase of the polymers' molecular weight (Table 1). On the basis of the approximate number of repeating units in the macroinitiators **P2a**−**c**, and assuming low polydispersity of the PNIPAm-grafted side chains (which is a signature feature of "living" ATRP polymerization), one could estimate number-average molecular weight (M_n) of a side chain in **P3a**−**c** to be around 3.5 kDa. The grafted polymers were found to be thermally stable in solid state and showed no thermal decomposition upon heating to ~320 °C as was revealed by TGA studies (Figure S1 in Supporting Information). Not surprisingly, solid vacuum-dried polymer samples contained about 8 wt % of water, likely entrapped within the PNIPAm grafted chains. Loss of this water accounted for the experimentally observed ~10% weight reduction upon heating the solid samples in the range of 25−150 °C in TGA experiments; the total weight loss was in good agreement with the water content obtained independently by Karl Fischer titration. Interestingly, at the temperatures above the decomposition point, the polymers showed rapid weight loss of almost 80% of the initial weight, possibly through depolymerization of the grafted side chains.

Table 1. Number-Average Molecular Weight, Polydispersity, and Regioregularity of Macroinitiators P2 and PNIPAm-Grafted Copolymers P3

polymer	M_n	D	% HT[a]
P2a	8000[b]	1.32	65
P2b	12000[b]	1.55	89
P2c	12000[b]	1.56	92
P3a	1.16×10^5 [c]	1.54	65
P3b	1.46×10^5 [c]	1.46	89
P3c	1.71×10^5 [c]	1.71	92

[a] Determined by ^{1}H NMR. [b] Determined by GPC in THF relative to polystyrene standards. [c] Determined by GPC in DMF using multiangle light scattering method.

Table 2. Spectral Properties of Polymers P2 and P3

	solution[a]				thin film[b]	
	in THF		in H_2O			
polymer	λ_{abs}, nm	λ_{em}, nm (Φ, %)	λ_{abs}, nm	λ_{em}, nm (Φ, %)	λ_{abs}, nm	λ_{em}, nm
P2a	417	549 (10)			435	580
P2b	415	559 (6)			510	641
P2c	434	566 (6)			520	638
P3a	415	536 (28)	430	545 (9)	422	546
P3b	425	544 (31)	457	573 (4)	445	564
P3c	433	547 (32)	476	573 (4)	461	571

[a] At 20 °C. [b] Obtained by spin-casting from THF solution.

Photophysical Properties of the Polymers. The PNIPAm-grafted copolymers **P3a**−**c** showed excellent solubility in water as well as in a variety of organic solvents (such as THF, chlorinated solvents, alcohols, etc.). At the same time, they were completely insoluble in aromatic solvents (toluene) and saturated hydrocarbons. As expected, increasing regioregularity from **P2a** to **P2c** (and from **P3a** to **P3c**) resulted in pronounced bathochromic shifts in the absorption and fluorescence spectra acquired in dilute THF solutions within each series (Table 2 and Figure 2).[13b,19] The PNIPAm grafting in copolymers **P3a**−**c** did not seem to have profound impact on the polymers' backbone conformation and did not affect their electronic spectra in dilute THF solutions. Indeed, each pair of the macroinitiator precursor **P2** and the corresponding PNIPAm-grafted copolymer **P3** featured very similar absorption and fluorescence spectra. However, PNIPAm grafting resulted in major increase in the fluorescence quantum yield (from around 10% in **P2a**−**c** to near 30% in **P3a**−**c**, Table 2). Increasing fluorescence efficiency likely reflects good "insulating" properties of the PNIPAm grafts which reduce exposure of the PT backbone to solvent molecules and prevent vibrationally coupled radiationless deactivation of the excited state.

Both absorption and fluorescence spectra of grafted copolymers **P3a**−**c** acquired in aqueous solution were bathochromically shifted with respect to the same spectra in THF solution (Table 2). The magnitude of the shift was relatively small (~15 nm) for regiorandom copolymer **P3a** but was much larger (30−40 nm) for regioregular copolymers **P3b** and **P3c**. The bathochromic shifts likely reflect increasing conjugation length of the PT backbone in aqueous medium.

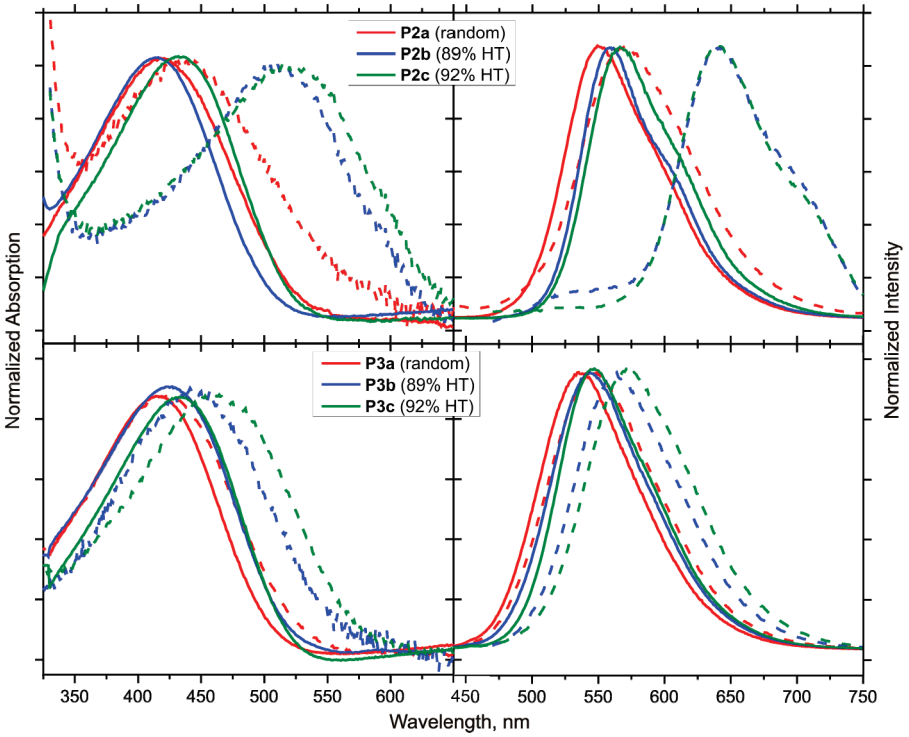

Figure 2. Absorption and fluorescence spectra of precursor polymers **P2a**−**c** (top) and PNIPAM-grafted copolymers **P3a**−**c** (bottom). Solid traces correspond to solution data and dashed traces to spin-cast films (prepared from THF solutions). Solution spectra were acquired at 20 °C in THF; concentration of all solutions was 0.15 mg mL^{-1}.

Presumably, hydrophilic PNIPAm side chains benefit from strong stabilizing interactions with water molecules in the extended coil conformation and impose a more planarized PT backbone with longer conjugation length.

The most striking difference between macroinitiator precursors **P2** and PNIPAm-grafted copolymers **P3** was found upon comparing their spin-cast film spectra. As expected, macroinitiators **P2** showed very significant aggregation in solid state, which resulted in large bathochromic shifts in absorption and fluorescence spectra and dramatic decrease of emission intensity. Such intermolecular aggregation is typical for soluble PTs and has been observed for polymers with a broad range of different substituents. Although all three precursor polymers **P2a**−**c** were substantially affected by intermolecular electronic interactions in solid films, the extent of such interactions was heavily dependent on the backbone regioregularity. The regioregular polymers **P2b** and **P2c** showed stronger tendency toward interchain aggregation due to the higher planarity of their conjugated backbones, while regiorandom polymer **P2a** showed much less pronounced aggregation-related spectroscopic changes in its spin-cast film (Figure 2). In stark contrast to macroinitiators **P2a**−**c**, PNIPAm-grafted copolymers **P3a**−**c** demonstrated practically no aggregation-related intermolecular electronic interactions in solid films prepared by spin-casting from THF solutions (Table 2 and Figure 1). This could be attributed to the presence of PNIPAm-grafted side chains which effectively "insulate" individual PT molecules and prevent interchain electronic communication upon aggregation in thin films. Depending on regioregularity of the PT backbone, small bathochromic shifts (relative to THF solution spectra) were observed in thin film spectra; the magnitude of the shifts was increasing with the increasing regioregularity. Remarkably, for each polymer **P3a**−**c** the magnitude of the bathochromic shift observed in spin-cast film spectra was similar to that of the spectra in aqueous solutions where it originated from enhanced backbone planarization (vide supra). It was likely that polymer backbone planarization (and possibly some supramolecular organization) also occurred upon spin-casting, thus resulting in more extended π-electron conjugation; the extent of planarization was consistent with the degree of regioregularity of the PT backbone.

To further assess the "insulating" role of the PNIPAm-grafted side chains in reducing interchain electronic interactions, a series of experiments were carried out in which the changes in the optical properties of PNIPAm-grafted polymers **P3** were followed at different extents of aggregation. These studies can be performed by creating stable solutions of nanoscopic nonscattering particles, thereby allowing quantitative studies of the polymer optical properties in aggregated state.[20] This was accomplished by adding various amounts of toluene ("bad" solvent) to methanol ("good" solvent) solutions of the grafted copolymers **P3** while keeping constant the polymer concentration in the final solutions (Figure 3). The aggregated particles of both regioregular and regiorandom grafted copolymers displayed no appreciable changes in absorption spectra and showed only minor changes (small intensity decrease along with a slight bathochromic emission band shift, possibly due to PT backbone planarization occurring upon aggregation as discussed above). In contrast, the "noninsulated" precursor polymers **P2** showed dramatic aggregation-related spectral changes as quality of solvent was gradually decreased (Figure 3; "good" solvent: chloroform; "bad" solvent: methanol). These spectral changes were found to be in agreement with the solution and thin-film spectral data for these polymers (Figure 2). Thus, it can be concluded that, owing to the "insulated" nature of the grafted copolymers **P3**, their spectral response in dilute solutions would be primarily due to the properties of individual isolated conjugated chains, with only minor (if any) influence of intermolecular electronic interactions.

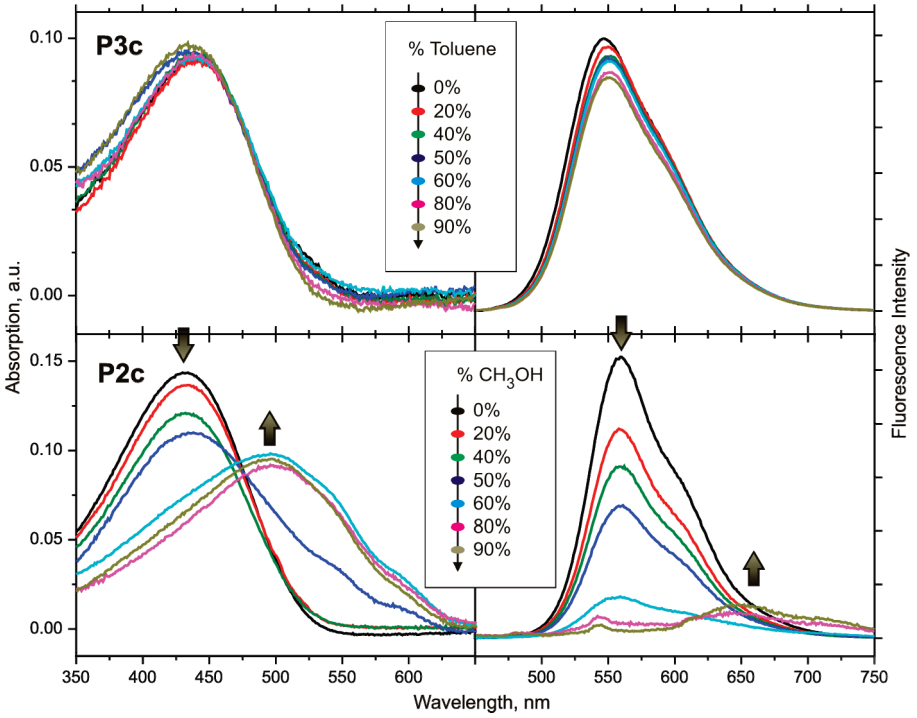

Figure 3. Absorption and fluorescence spectra of polymers **P3c** (top row) and **P2c** (bottom row) acquired at 20 °C in "good"−"bad" solvent mixtures with increasing fraction of a "bad" solvent ("good" solvent: methanol for **P3c** and chloroform for **P2c**; "bad" solvent: toluene for **P3c** and methanol for **P2c**).

Temperature-Dependent Spectroscopic Properties. All three grafted copolymers **P3a**−**c** exhibited temperature-induced spectral changes in dilute solutions which were consistent with the idea of the PT backbone conformational switching when grafted PNIPAm side chains collapse into globular phase at the temperatures above LCST. These changes included pronounced hypsochromic absorption and fluorescence spectral shifts as well as intensity increase of fluorescent emission upon heating the solutions (Figure 4); these spectral changes were found to be completely reversible upon cooling the solutions. The magnitude of changes was strongly dependent on the extent of regioregularity of PT conjugated backbone, with random copolymer **P3a** displaying only small changes (consistent with previous observation by McCarley et al.[11]) and regioregular polymers showing much more pronounced changes. Thus, the highest regioregularity polymer **P3c** showed a 20 nm hypsochromic shift in absorption maximum as well as 16 nm shift in emission maximum when temperature was increased from 20 to 50 °C, whereas the regiorandom polymer **P3a** displayed only smaller 8 nm absorption and emission shifts. The more pronounced spectral changes in regioregular polymer **P3c** were consistent with the notion of more planarized backbone conformation of this polymer in dilute solutions, which potentially allows larger conformational changes toward backbone twisting, in contrast to the regiorandom copolymer **P3a**. Surprisingly, two regioregular copolymers **P3b** and **P3c** showed strikingly different thermochromic behavior despite only a small 3% difference in regioregularity (Figure 5). Clearly, the effect of conjugated backbone regioregularity on the extent of PT conformational twisting was not linear, and the relatively small increase in regioregularity could lead to dramatic effect on the ease and magnitude of the conformational twisting.

Although thermochromism (temperature-induced spectral changes) is a well-documented phenomenon found both for solutions and thin films of regiorandom and regioregular

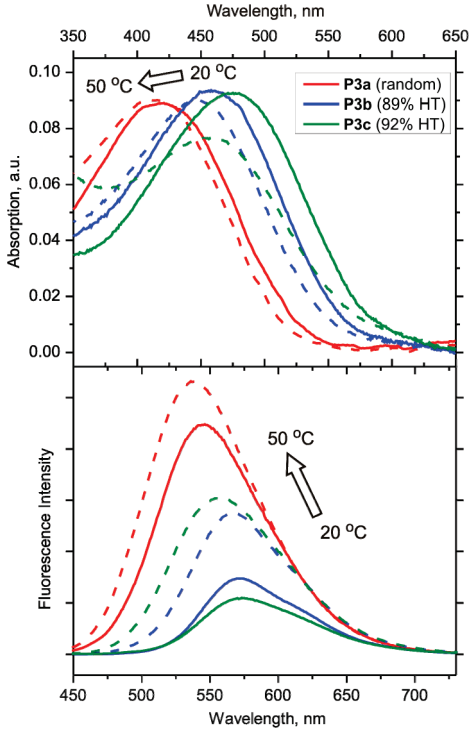

Figure 4. Absorption (top) and fluorescence (bottom) spectra of PNIPAm-grafted copolymers **P3a**−**c** in aqueous solution (concentration 0.15 mg mL^{-1}) at 20 °C (solid traces) and 50 °C (dash traces). The spectra are not normalized for intensity comparison purposes.

PTs, it generally occurs in a much wider (≥100 °C) range of temperatures and is related to conformation-induced intermolecular aggregation, resulting in appearance of a new distinct absorption band; in many instances it is irreversible.[21] In contrast, the presently observed thermochromic

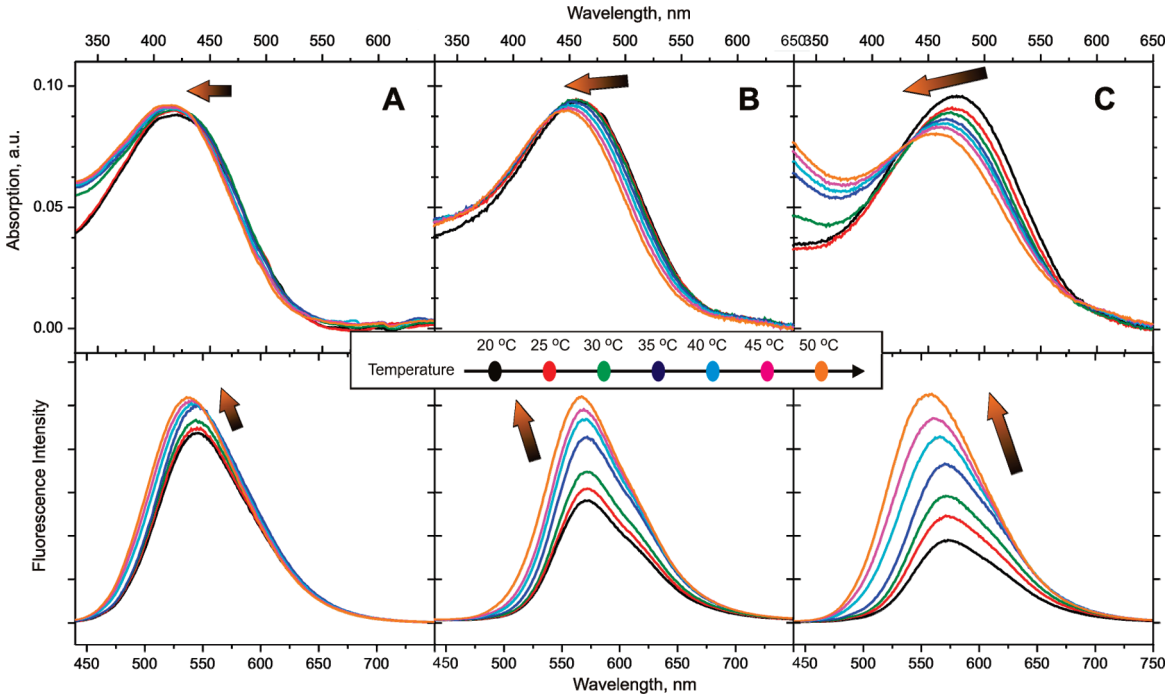

Figure 5. Temperature-dependent absorption (top row) and corresponding fluorescence (bottom row) spectra of PNIPAm-grafted copolymers **P3a** (A), **P3b** (B), and **P3c** (C) in aqueous solution (concentration 0.15 mg mL^{-1}).

Table 3. Fluorescence Lifetimes of Polymer P3c in Aqueous Solution[a]

temp (°C)	τ_1 (ns)[b]	τ_2 (ns)[b]	χ^2
20	0.56 (0.90)	3.18 (0.10)	0.95
50	0.51 (0.92)	3.34 (0.08)	0.79

[a] Concentration 0.20 mg mL^{-1}. [b] Pre-exponential amplitude is given in parentheses (to add to 1.00).

behavior is completely different in nature and appearance as it originates from the reversible conformational switching of isolated conjugated polymer chains in a relatively narrow temperature interval. As such, it only results in spectral wavelength shifts, without appearance of a new absorption band. Indeed, the presently observed hypsochromic shifts upon heating solution of the regioregular copolymer **P3c** were very similar to those found by Kim and Swager for a surface-pressure-induced planar to perpendicularly twisted conformational transition of poly(*p*-phenylene ethynylene)s (PPEs) in Langmuir monolayer.[22] Although some caution should be exercised when drawing parallels between PTs and PPEs, extended π-electron conjugated nature of the planarized conformation of both classes of polymers makes such comparison viable.

Further support in favor of the conformational switching was obtained from fluorescence lifetime measurements in dilute aqueous solution of **P3c** using the phase modulation technique. Both at 20 and 50 °C, the polymer emission decay was found to be double-exponential (Table 3), likely indicating the presence of two independent decay pathways. The major, short-lived component showed values typical for PT polymers; the decrease from 0.56 ns at 20 °C to 0.51 ns at 50 °C was consistent with formation of a more twisted, less conjugated PT conformation at higher temperature.[23] This also paralleled the previous observations of a similar lifetime decrease in the more twisted, lower conjugation length conformations of PPEs[4d] and their small-molecule congener.[24] Increasing pre-exponential amplitude of the short-lived decay component was also in agreement with the increasing role of the short-lived decay pathway due to conformational twisting. The origin of the minor 3 ns decay component is not particularly clear. In many cases, the presence of a long-lived component indicates formation of exciplex-like species due to intermolecular aggregation.[25] However, the possibility of such electronic interactions seemed unlikely considering the "insulating" nature of the PNIPAm grafted side chains. Also, the relative contribution of the long-lived decay pathway consistently *decreases* with increasing temperature (Table 3), which contradicts the data obtained from dynamic light scattering experiments (vide infra) that clearly indicate an *increase* in intermolecular aggregation as the temperature traverses through LCST. If intermolecular interactions are ruled out, and we assume that both decay components originate from isolated individual polymer chains, it could be possible that the short-lived component is associated with the fast coherent Dexter energy migration mechanism, while the long-lived component originates from the long-range incoherent exciton hopping.[26] In such case, the predominance of the short-lived component, especially at the higher temperature, does signify appreciable role of the conformation-dependent through-bond exciton migration process.

The diminished conjugation length due to temperature-induced PT backbone twisting was also consistent with an almost 3-fold increase of emission intensity of **P3c** observed upon increasing the temperature from 20 to 50 °C (Figure 5C). This was probably due to the shortening exciton diffusion length in the twisted conformation, which reduced the probability of excited state quenching with residual impurities or backbone defects. In contrast to PNIPAm-grafted copolymers, the precursor polymers **P2a**−**c** showed only subtle spectral changes when their THF solutions were studied in the same 20−50 °C temperature range (Figure S2 in Supporting Information), thus further supporting the uniqueness of the temperature-induced backbone conformational twisting in grafted copolymers **P3a**−**c**. Similarly, no substantial spectral changes were observed when THF was

used instead of water as a solvent for grafted copolymers **P3a**−**c** (Figure S3 in Supporting Information). Because the PNIPAm phase transition does not happen in THF, increasing temperature alone did not cause conformational twisting of the PT backbone in **P3a**−**c**; this emphasizes the critical role of the grafted PNIPAm side chains phase transition in the observed temperature-induced spectral changes.

Since the PNIPAm phase transition occurs in a narrow temperature range around LCST, one would expect relatively sharp threshold change in the copolymers **P3a**−**c** spectral properties when the temperature traverses through LCST. Such threshold change occurring between 30 and 35 °C could indeed be observed in the case of regiorandom copolymer **P3a** (Figure 5A). However, in the increasingly more regioregular copolymers **P3b** and **P3c**, the change was found to become more continuous and spread over a broader temperature interval. Whereas some threshold change could still be noticed in the copolymer **P3b** (89% HT), it became completely continuous for the copolymer **P3c** (92% HT) (Figure 5B,C). Thus, continuity of the temperature-induced spectral changes was strongly dependent on regioregularity of the PT backbone. Since neither parent precursor polymers **P2a**−**c** nor PNIPAm-grafted copolymers **P3a**−**c** showed appreciable temperature-dependent spectral changes in THF solution, it was the PNIPAm phase transition in aqueous medium which had to be responsible for the conformational changes and observed spectral changes in the copolymers **P3a**−**c**. To gain deeper understanding of the continuous change phenomenon, differential scanning calorimetry (DSC) studies on dilute solutions of the copolymers **P3a**−**c** were carried out. The DSC experiments revealed that the PNIPAm phase transition occurred reversibly upon heating and cooling in the narrow temperature interval around LCST in all three grafted copolymers, independent of their regioregularity; this transition was associated with narrow endothermic (heating) and exothermic (cooling) peaks (Figure 6). An additional broad peak partially overlapping with the main narrow peak and corresponding to a phase transition in the 32−45 °C temperature range was particularly noticeable in DSC data for the copolymer **P3c**. This peak was found to be less pronounced (but still present) in DSC data for the less regioregular copolymer **P3b** and was seemingly absent in the case of regiorandom polymer **P3a** (Figure 6). The presence of this additional phase transition in solutions of regioregular grafted copolymers was an important feature likely related to the temperature-induced continuous spectral changes in these polymers.

Important information about temperature-dependent behavior of the copolymers **P3a**−**c** was obtained from small-angle dynamic light scattering (DLS) studies. Analysis of DLS data (Figure 7) revealed interesting temperature-induced features. Both regiorandom and regioregular copolymers **P3a** and **P3c** at 20 °C showed similar diffusion coefficients (around $(1.2-1.3) \times 10^{-11}$ m^2 s^{-1}). Increasing temperature from 20 to 32 °C resulted in gradual and almost linear increase of the diffusion coefficients up to $\sim 2 \times 10^{-11}$ m^2 s^{-1}. This increase can be associated with a continuous precollapse of the extended coils of PNIPAm grafted chains,[18c] which decreases the polymer's radius of gyration and increases the apparent diffusion coefficient. Such "continuous" precollapse of grafted PNIPAm side chains before the "precipitous" collapse at LCST was previously reported[27] and would result in increasing the effective steric size of the PNIPAm substituents in the vicinity of the PT conjugated backbone. Therefore, it can be responsible for the continuous, gradual temperature-dependent PT backbone conformational twisting found for the regioregular

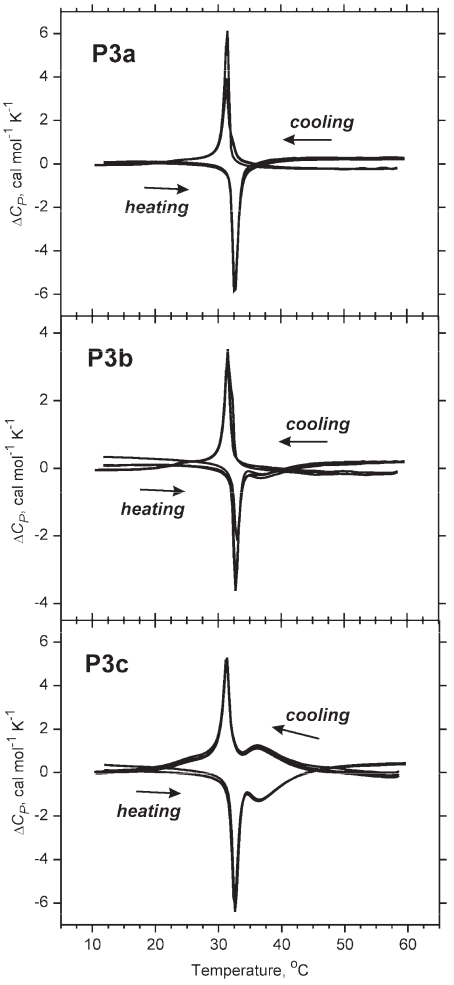

Figure 6. DSC data for PNIPAM-grafted copolymers **P3a**−**c** in aqueous solution (concentration 0.25 mg mL^{-1}). Three repeated cycles of heating and cooling are shown for each polymer.

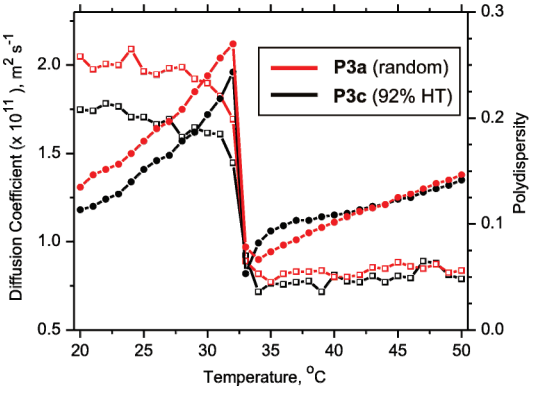

Figure 7. Temperature-dependent small-angle DLS data for PNIPAm-grafted copolymers **P3a** and **P3c** in aqueous solution (concentration 0.5 mg mL^{-1}). Traces marked with solid circles use left *Y*-axis and represent diffusion coefficients; traces marked with squares use right *Y*-axis and correspond to DLS "polydispersity".

copolymers **P3b** and **P3c** at the temperatures below LCST.[28] The enhanced intermolecular interactions between PNIPAm-grafted side chains attached to the PT backbone in regioregular fashion were likely to intensify and "expand" the precollapse over longer temperature range, which explains the significant continuous spectral changes in regioregular copolymer **P3c** observed at the temperatures below

LCST, in contrast to only the subtle changes in the regiorandom copolymer **P3a** (Figure 5).

Upon further heating, a sharp drop in diffusion coefficients was observed for both **P3a** and **P3c** copolymers in the very narrow 32−33 °C temperature range. Since this event occurred at exactly the same temperature as the major phase transition found in DSC studies (vide supra), it could be assigned to the extended coil−collapsed globule PNIPAm phase transition at LCST. It coincided with the threshold spectral changes observed in solution of the regiorandom polymer **P3a** (and, to some extent, in polymer **P3b**) originating from the backbone conformational twisting. From general considerations, the PNIPAm phase transition from extended coil to collapsed globule at LCST was expected to diminish the effective size (radius of gyration) of an individual molecule and *increase* the diffusion coefficients. Thus, experimentally observed sharp *decrease* in diffusion coefficients at LCST surprisingly contradicted this assumption. Very likely, this drop reflected formation of intermolecular aggregates upon the PNIPAm grafted side chains precipitous collapse. The idea of loose aggregate formation is also in agreement with a sharp drop of DLS "polydispersity" from the values around 0.2−0.25 before LCST to 0.05 at the temperatures above this point (Figure 7). The aggregate formation in aqueous solutions at the temperatures above LCST is driven by increasing hydrophobicity of the collapsed globule phase and is well-documented for PNIPAm polymers.[9] Because of the relatively short size of conjugated PT backbone in the present study (30−40 thienyl repeating units) and relatively large size of PNIPAm-grafted side chains, it was unlikely that any noticeable folding of the PT chains could happen upon aggregation; it is more likely that the individual polymer chains formed loose side-by-side aggregates in their elongated wormlike conformation. Furthermore, these aggregates were likely to consist of only a small number of individual polymer molecules. Indeed, the calculated (using Stokes−Einstein equation[29]) average hydrodynamic radius of the scattering particles in solution changed from 30 nm just before reaching LCST to 60 nm at the temperatures slightly above LCST. Even taking into account the very qualitative nature of this estimation (since the polymer particles could not be perfectly spherical), it would be safe to suggest that an average aggregate included no more than three polymer molecules. As discussed above, such loose intermolecular aggregation could not directly affect the electronic properties of the copolymers **P3a−c** due to the PNIPAm grafts acting as efficient "insulator" for the conjugated PT backbone. It, however, could affect the conformation of the conjugated backbone as individual polymer chains would have to accommodate each other within the aggregated state.

Interestingly, further temperature rise from 33 to 50 °C resulted in growing effective diffusion coefficients as the polymer aggregates accommodated into more optimal intermolecular packing with decreasing overall dimensions. The increase was almost linear for the regiorandom copolymer **P3a**; however, it showed a much steeper, almost exponential increase in the 33−45 °C temperature range for the regioregular copolymer **P3c** (Figure 7). This temperature range perfectly coincided with the temperature range where a second broad phase transition was observed for the aqueous **P3c** solution in DSC experiments (Figure 6). On the basis of this observation, we hypothesize that this broad transition corresponds to the PT backbone conformational twisting as individual polymer chains try to better accommodate each other within the aggregates; this explains the observed continuous spectral change for **P3c** in aqueous solution at the temperatures above LCST (Figure 5). Although it was not possible a priori to anticipate that such a seemingly minor factor would cause such a significant conformational twisting of the regioregular polymer (of almost the same magnitude as the conformational change caused by the phase transition of grafted PNIPAm side chains), it can be easily understood considering the small energy required for twisting the regioregular PT backbone.

Conclusions

Reversible temperature-induced control of conjugated backbone conformation and conjugation length was demonstrated using a series of PNIPAm-grafted water-soluble fluorescent PTs. The grafted PNIPAm side chains provide an efficient "insulation" of the conjugated backbone, so the effect of intermolecular electronic interactions is greatly diminished to allow studies of the properties of electronically isolated CP molecules. The temperature-induced phase transition of the grafted side chains was responsible for the conformational twisting of the conjugated backbone at rising temperature, resulting in decreasing conjugation length, hypsochromic shifts in absorption and emission spectra, and increasing intensity of fluorescent emission along with a small drop in emission lifetime. The extent of the temperature-induced conformational switching, as well as the magnitude and nature of spectroscopic changes, was found to be strongly dependent on the degree of regioregularity of the PT backbone. A regiorandom copolymer showed relatively small changes, which mostly occurred in a narrow temperature range around 32 °C corresponding to the PNIPAm phase transition. In contrast, regioregular polymers showed much greater spectral changes which occurred continuously in the temperature interval significantly exceeding that of the PNIPAm phase transition range. The effect of regioregularity was clearly not linear, as only a small increase in regioregularity (from 89% to 92%) led to very substantial difference in the extent of conformational switching. The enhanced continuous conformational and spectral changes in regioregular polymers are likely to be related to side-group-driven aggregation, as was supported by the results of thermal and light-scattering experiments. It is possible that the PNIPAm-grafted copolymers of even higher regioregularity will demonstrate remarkably higher temperature-induced conformational switching control. Further experimental studies on the effect of regioregularity and other factors capable of influencing this behavior as well as gaining a deeper understanding of the nature and origin of this phenomenon are required and are currently underway.

Experimental Section

General Procedures. All reactions were performed under an atmosphere of dry nitrogen. Column chromatography was performed on silica gel (Sorbent Technologies, 60 Å, 40−63 μm) slurry packed into glass columns. Tetrahydrofuran (THF) was dried by passing through activated alumina and *N,N*-dimethylformamide (DMF) by passing through activated molecular sieves, using a PS-400 solvent purification system from Innovative Technology, Inc. The water content of the solvents was periodically controlled by Karl Fischer titration (using a DL32 coulometric titrator from Mettler Toledo). All other reagents and solvents were obtained from Aldrich and Alfa Aesar and used without further purification. ^{1}H NMR spectra were recorded at 250 and 400 MHz and are reported in ppm downfield from tetramethylsilane. UV−vis spectra were recorded on Varian Cary 50 UV−vis spectrophotometer supplied with a temperature-controlled multicell holder. Fluorescence studies were carried out with a PTI QuantaMaster4/2006SE spectrofluorimeter equipped with a water-heated cell holder connected to a Neslab RTE-7 thermostat for variable-temperature experiments.

Fluorescence quantum yields were determined using ethanol solutions of Coumarin 6 ($\Phi = 0.78$[30]) as standard. Thermogravimetric analysis (TGA) of solid polymer samples was performed using TGA 2950 from TA Instruments (New Castle, DE) at a heating rate of 10 °C min^{-1} in a nitrogen atmosphere. Differential scanning calorimetry (DSC) experiments were performed on a MicroCal VP-DSC. Buffer baselines were subtracted to obtain the excess heat capacity curves, which were analyzed using the manufacturer supplied MicroCal Origin DSC Software, Version 5.0. GPC analyses of precursor polymers **P1** and **P2** were performed with Agilent 1100 chromatograph equipped with two PLgel 5 μm MIXED-C and one PLgel 5 μm 1000 Å columns connected in series, using THF as a mobile phase, and calibrated against polystyrene standards. GPC data for copolymers **P3** were acquired with an Agilent 1200 chromatograph equipped with three Phenogel 5 μm 300 × 7.8 mm columns (100 Å, 1000 Å, and Linear(2)) connected in series, using 0.1 M LiBr solution in DMF as a mobile phase, and equipped with a Wyatt DAWN EOS multiangle light scattering detector. The specific refractive angle increment (dn/dc) was measured using a series of polymer solutions in 0.1 M LiBr in DMF with different polymer concentrations using a Wyatt Optilab rEX differential refractometer (experimental dn/dc 0.057 ± 0.002). Thin-film polymer samples were spin-casted at 1500 rpm from 1 mg mL^{-1} THF solutions using Laurell Technologies WS-400B-6NPP spin processor. Water content in polymers **P3a**−**c** was determined by dissolving a vacuum-dried polymer sample in anhydrous dichloromethane (water content 1.8 ppm) with subsequent Karl Fischer titration using a DL32 coulometric titrator (Mettler Toledo).

Dynamic Light Scattering (DLS) Measurements. DLS measurements were carried out with a Zetasizer nano ZS instrument (Malvern Instruments, Malvern, U.K.). This system is equipped with a 4 mW He/Ne laser at a wavelength of 632.8 nm and measures the particle size using noninvasive backscattering at a detection angle of 173°. Temperature (20−50 °C) was controlled by the instrument (thermoelectric cooling/heating).

At least 12 measurements of the correlation time of scattered light intensity, $G(\tau)$, were averaged for each sample. The data were fitted to eq 1, where B is baseline, A is amplitude, q is the scattering vector, τ is delay time, and D is the diffusion coefficient:

$$G(\tau) = B + Ae^{-2q_2D\tau} \quad (1)$$

The hydrodynamic radius (R_H) of the scattering particles is inversely proportional to the diffusion coefficient D and the solvent viscosity (η), as shown in the Stokes−Einstein equation (eq 2), where k_B is Boltzmann's constant and T denotes the absolute temperature:

$$R_H = \frac{k_B T}{6\pi\eta D} \quad (2)$$

Frequency-domain lifetime fluorescence measurements were performed using a Spex Fluorolog-3 spectrofluorimeter (model FL3-22TAU3; HORIBA Jobin Yvon, Edison, NJ). Fluorescence decay times were measured using a variable frequency phase-modulation technique. The system used 450 W Xe arc lamp light source and Hamamatsu R928 PMT detector operating at 950 V. Full-sized 1 cm quartz cells were placed in a carousel thermostated cell holder and used with 450 nm excitation. The emission was collected through a 500 nm long pass filter. Thirty-eight logarithmically spaced frequencies were collected over a frequency range of 10−174.6 MHz using five averages and a 10 s integration time at each frequency. Frequency-domain measurements were collected versus Ludox, a scatter reference solution, which showed lifetime of 0 ns. Constant phase and modulation errors of 0.5° and 0.005 were used in analyses for consistency and ease of day-to-day data interpretation.

Synthetic Details. *2,5-Dibromo-3-(2-hydroxyethyl)thiophene*. NBS (6.75 g, 37.9 mmol) was added in a few small portions over period of 30 min to a stirred at 0 °C solution of 4.82 g (37.6 mmol) of 2-(3-thienyl)ethanol (**1**) in 50 mL of THF. After the addition was completed, the reaction mixture was stirred at 0 °C for 2 h, poured into water, extracted with diethyl ether (3 × 50 mL), washed with water, and dried over Na_2SO_4. The resulting solution was filtered through a short plug of silica gel eluted with ether and concentrated in vacuo to afford 6.0 g (56%) of the target product as yellowish oil. The ^{1}H NMR data were consistent with those published in literature.[31]

2-[(2,5-Dibromothiophen-3-yl)ethyloxy]-tert-butyldimethylsilane (**2**). Imidazole (4.9 g, 73.0 mmol) was added to a solution of 6.0 g (21.0 mmol) of 2,5-dibromo-3-(2-hydroxyethyl)thiophene in 60 mL of DMF, and the resulting mixture was stirred at room temperature for 15 min. This was followed by addition of 5.2 g (34.4 mmol) of TBDMS-Cl in 10 mL of DMF. The reaction mixture was stirred for 16 h at room temperature, poured into water−ice mixture, and extracted with hexane (3 × 60 mL); the organic fraction was washed with water and dried over Na_2SO_4. Concentration in vacuo afforded crude product which was purified by column chromatography on silica gel (eluent hexane−EtOAc 3:1) to yield 8.0 g (95%) of **2** as colorless oil, R_f 0.80. ^{1}H NMR (250 MHz, $CDCl_3$): δ 6.85 (s, 1H), 3.75 (t, J = 6.8 Hz, 2H), 2.75 (t, J = 6.8 Hz, 2H), 0.85 (s, 9H), 0.01 (s, 6H).

*Polymer **P1b***. A solution of *tert*-BuMgCl (1.25 mL of 1.0 M solution in THF, 1.25 mmol) was added dropwise to a solution of 0.5 g (1.25 mmol) of **2** in 20 mL of THF, and the resulting mixture was stirred at reflux conditions for 2 h. A catalytic amount of Ni(dppp)Cl_2 (6 mg) was added in one portion, and the reaction mixture was stirred at reflux conditions for 20 h. Precipitation into 120 mL of methanol resulted in a dark-red polymer which was placed into a Soxhlet extractor and extracted successively with methanol, hexane, and $CHCl_3$. The chloroform fraction yielded 0.12 g (40%) of **P1b** as dark-red solid material; M_n (GPC, vs polystyrene) 12 000, D 1.55. ^{1}H NMR (400 MHz, $CDCl_3$): δ 7.02 (s, 1H), 3.89 (s, 2H), 2.99 (s, 1.78 H), 2.80 (s, 0.22 H) 0.99 (s, 9H), 0.0 (s, 6H).

*Polymer **P1c*** was prepared following the procedure for polymer **P1b**.

*Regiorandom polymer **P1a*** was prepared following the same procedure but using a catalytic amount of Ni$(PPh_3)_2Cl_2$ instead of Ni(dppp)Cl_2. M_n (GPC, vs polystyrene) 8000, D 1.32. ^{1}H NMR (400 MHz, $CDCl_3$): δ 7.02 (br s, 1H), 3.81 (two overlapping br s, 2H), 2.99 (br s, 1.29 H), 2.76 (br s, 0.71 H), 0.86 (s, 9H), 0.07 (s, 6H).

*Polymer **P2b***. A solution of Bu_4NF (2.6 mL of 0.1 M solution in THF, 0.26 mmol) was added dropwise over the period of 2 h (syringe pump) to a mixture of 50 mg (0.21 mmol) of polymer **P1b**, 0.48 g of 2-bromoisobutyryl bromide (0.26 mL, 2.1 mmol), and 36 μL of triethylamine (0.26 mmol) in 20 mL of THF at room temperature, and the resulting mixture was stirred at room temperature for 16 h. Precipitation into methanol and washing with acetone yielded 45 mg (79%) of **P2b** as dark-red solid material, M_n (GPC, vs polystyrene) 12 000, D 1.55. ^{1}H NMR (400 MHz, $CDCl_3$): δ 7.17 (s, 1H), 4.47 (s, 2H), 3.23 (s, 1.79 H), 3.03 (s, 0.21 H), 1.93 (s, 6H).

*Polymers **P2a** and **P2c*** were prepared exactly following the procedure for **P1b** starting from **P1a** and **P1c**, respectively. **P2a**: M_n (GPC, vs polystyrene) 8000, D 1.32. ^{1}H NMR (400 MHz, $CDCl_3$): δ 7.16 (br s, 1H), 4.40 (two overlapping br s, 2H), 3.23 (br s, 1.34 H), 3.00 (br s, 0.66 H), 1.93 (s, 6H). **P2c**: M_n (GPC, vs polystyrene) 12 000, D 1.55. ^{1}H NMR (250 MHz, $CDCl_3$): δ 7.17 (s, 1H), 4.48 (s, 2H), 3.23 (s, 1.85 H), 3.03 (s, 0.15 H), 1.93 (s, 6H).

*Polymer **P3b***. An air-free flask was charged with 20 mg (0.14 mmol) of CuBr, 1.5 g (13.3 mmol) of *N*-isopropylacrylamide, and 31 mg (0.12 mmol) of 1,4,8,11-tetramethyl-1,4,8,11-tetraazacyclotetradecane, evacuated and backfilled with Ar 3 times, filled with 10 mL of THF, cooled in an ice bath, and purged with Ar for 10 min. After 15 min, a separately prepared and degassed

in an air-free flask solution of 40 mg (0.14 mmol based on repeating unit) of **P2b** in 35 mL of THF was added dropwise via cannula. The resulting mixture was stirred at 0 °C for 2.5 h, and then it was poured into 200 mL of hexane to precipitate a crude polymer product. The precipitate was washed twice with diethyl ether, redissolved in THF, and precipitated into hexane. Finally, this precipitate was redissolved in THF and filtered through a short plug of silica gel eluted with THF to remove catalyst. The THF solution was again precipitated from hexane and dried in vacuo to afford 0.9 g of **P3b** as bright yellow solid material, M_n (GPC using light-scattering detector) 1.46×10^5, D 1.46, water content (by Karl Fischer titration) 10.2 wt %. ^{1}H NMR (250 MHz, $CDCl_3$): δ 6.8−6.2 (br s, 1H), 3.98 (br s, 1H), 2.47 (br s, 1H), 2.20−1.62 (br m, 2H) 1.13 (s, 6H).

*Polymers **P3a** and **P3c*** were prepared following the same procedure starting from **P2a** and **P2c**, respectively. **P3a**: M_n (GPC using light-scattering detector) 4.54×10^5, D 1.88, water content (by Karl Fischer titration) 12.0 wt %. **P3c**: M_n (GPC using light-scattering detector) 1.71×10^5, D 1.71, water content (by Karl Fischer titration) 9.4 wt %. ^{1}H NMR spectra for **P3a** and **P3c** were similar to that of **P3b**.

Acknowledgment. This research was supported by the National Science Foundation (CAREER Award CHE-0547895). Kind appreciation is due to Dr. Rafael Cueto for invaluable help with DLS experiments and TGA analysis, Prof. Vince J. LiCata for DSC studies, and Dr. Santhosh Challa for helping with phase-modulated lifetime measurements.

Supporting Information Available: ^{1}H NMR spectra for compounds **2** and **P1**−**P3** as well as additional data and figures. This material is available free of charge via the Internet at http://pubs.acs.org.

References and Notes

(1) (a) McQuade, D. T.; Pullen, A. E.; Swager, T. M. *Chem. Rev.* **2000**, *100*, 2537–2574. (b) Thomas, S. W., III; Joly, G. D.; Swager, T. M. *Chem. Rev.* **2007**, *107*, 1339–1386. (c) Swager, T. M. *Acc. Chem. Res.* **1998**, *31*, 201–207.

(2) (a) Bunz, U. H. F. *Chem. Rev.* **2000**, *100*, 1605–1644. (b) Chen, L.; McBranch, D. W.; Wang, H.-L.; Helgeson, R.; Wudl, F.; Whitten, D. G. *Proc. Natl. Acad. Sci. U.S.A.* **1999**, *96*, 12287–12292. (c) Finden, J.; Kunz, T. K.; Branda, N. R.; Wolf, M. O. *Adv. Mater.* **2008**, *20*, 1998–2002. (c) Zhao, X.; Jiang, H.; Schanze, K. S. *Macromolecules* **2008**, *41*, 3422–3428.

(3) (a) Schwartz, B. J. *Annu. Rev. Phys. Chem.* **2003**, *54*, 141–172. (b) Averbeke, B. V.; Beljonne, D. *J. Phys. Chem. A* **2009**, *113*, 2677–2682. (c) Collini, E.; Scholes, G. D. *Science* **2009**, *323*, 369–373. (d) Nesterov, E. E.; Zhu, Z.; Swager, T. M. *J. Am. Chem. Soc.* **2005**, *127*, 10083–10088.

(4) (a) Pinto, M. R.; Schanze, K. S. *Proc. Natl. Acad. Sci. U.S.A.* **2004**, *101*, 7505–7510. (b) Liu, B.; Bazan, G. C. *Chem. Mater.* **2004**, *16*, 4467–4476. (c) Kim, I.-B.; Erdogan, B.; Wilson, J. N.; Bunz, U. H. F. *Chem.—Eur. J.* **2004**, *10*, 6247–6254. (d) Wosnick, J. H.; Mello, C. M.; Swager, T. M. *J. Am. Chem. Soc.* **2005**, *127*, 3400–3405. (e) He, F.; Tang, Y.; Yu, M.; Wang, S.; Li, Y.; Zhu, D. *Adv. Funct. Mater.* **2006**, *16*, 91–94. (f) Jiang, H.; Zhao, X.; Schanze, K. S. *Langmuir* **2006**, *22*, 5541–5543. (g) Liu, B.; Bazan, G. C. *J. Am. Chem. Soc.* **2006**, *128*, 1188–1196. (h) Disney, M. D.; Zheng, J.; Swager, T. M.; Seeberger, P. H. *J. Am. Chem. Soc.* **2004**, *126*, 13343–13346.

(5) (a) Ho, H.-A.; Najari, A.; Leclerc, M. *Acc. Chem. Res.* **2008**, *41*, 161–178. (b) Ho, H. A.; Doré, K.; Boissinot, M.; Bergeron, M. G.; Tanguay, R. M.; Boudreau, D.; Leclerc, M. *J. Am. Chem. Soc.* **2005**, *127*, 12673–12676. (c) Nilsson, K. P. R.; Åslund, A.; Berg, I.; Nyström, S.; Konradsson, P.; Herland, A.; Inganäs, O.; Stabo-Eeg, F.; Lindgren, M.; Westermark, G. T.; Lannfelt, L.; Nilsson, L. N. G.; Hammarström, P. *ACS Chem. Biol.* **2007**, *2*, 553–560. (d) Sigurdson, C. J.; Nilsson, K. P. R.; Hornemann, S.; Manco, G.; Polymenidou, M.; Schwarz, P.; Leclerc, M.; Hammarström, P.; Wüthrich, K.; Aguzzi, A. *Nat. Methods* **2007**, *4*, 1023–1030. (e) Abérem, M. B.; Najari, A.; Ho, H.-A.; Gravel, J.-F.; Nobert, P.; Boudreau, D.; Leclerc, M. *Adv. Mater.* **2006**, *18*, 2703–2707. (f) Tang, Y.; He, F.; Yu, M.; Feng, F.; An, L.; Sun, H.; Wang, S.; Li, Y.; Zhu, D. *Macromol. Rapid Commun.* **2006**, *27*, 389–392. (g) Li, C.; Numata, M.; Takeuchi, M.; Shinkai, S. *Angew. Chem., Int. Ed.* **2005**, *44*, 6371–6374. (h) Nilsson, K. P. R.; Inganäs, O. *Nat. Mater.* **2003**, *2*, 419–424. (i) Béra-Abérem, M.; Ho, H.-A.; Leclerc, M. *Tetrahedron* **2004**, *60*, 11169–11173.

(6) (a) Wang, M.; Zou, S.; Guerin, G.; Shen, L.; Deng, K.; Jones, M.; Walker, G. C.; Scholes, G. D.; Winnik, M. A. *Macromolecules* **2008**, *41*, 6993–7002. (b) Hoeben, F. J. M.; Jonkheijm, P.; Meijer, E. W.; Schenning, A. P. H. J. *Chem. Rev.* **2005**, *105*, 1491–1546.

(7) (a) Beljonne, D.; Pourtois, G.; Silva, C.; Hennebicq, E.; Hertz, L. M.; Friend, R. H.; Scholes, G. D.; Setayesh, S.; Müllen, K.; Brédas, J. L. *Proc. Natl. Acad. Sci. U.S.A.* **2002**, *99*, 10982–10987. (b) Nguyen, T.-Q.; Wu, J.; Doan, V.; Schwartz, B. J.; Tolbert, S. H. *Science* **2000**, *288*, 652–656. (c) Wang, C. F.; White, J. D.; Lim, T. L.; Hsu, J. H.; Yang, S. C.; Fann, W. S.; Peng, K. Y.; Chen, S. A. *Phys. Rev. B* **2003**, *67*, 035202.

(8) (a) Mano, J. F. *Adv. Eng. Mater.* **2008**, *10*, 515–527. (b) Lyon, L. A.; Meng, Z.; Singh, N.; Sorrell, C. D.; St. John, A. *Chem. Soc. Rev.* **2009**, *38*, 865–874. (c) Jeong, B.; Kim, S. W.; Bae, Y. H. *Adv. Drug Delivery Rev.* **2002**, *54*, 37–51.

(9) Schild, H. G. *Prog. Polym. Sci.* **1992**, *17*, 163–249.

(10) (a) Uchiyama, S.; Matsumura, Y.; de Silva, A. P.; Iwai, K. *Anal. Chem.* **2003**, *75*, 5926–5935. (b) Creshaw, B. R.; Kunzelman, J.; Sing, C. E.; Andler, C.; Weder, C. *Macromol. Chem. Phys.* **2007**, *208*, 572–580. (c) Shiraishi, Y.; Miyamoto, R.; Hirai, T. *Langmuir* **2008**, *24*, 4273–4279.

(11) Balamurugan, S. S.; Bantchev, G. B.; Yang, Y.; McCarley, R. L. *Angew. Chem., Int. Ed.* **2005**, *44*, 4872–4876.

(12) (a) Loewe, R. S.; Khersonsky, S. M.; McCullough, R. D. *Adv. Mater.* **1999**, *11*, 250–258. (b) Loewe, R. S.; Ewbank, P. C.; Liu, J.; Zhai, L.; McCullough, R. D. *Macromolecules* **2001**, *34*, 4324–4333. (c) Osaka, I.; McCullough, R. D. *Acc. Chem. Res.* **2008**, *41*, 1202–1214. (d) Jeffries-El, M.; McCullough, R. D. Regioregular polythiophenes. In *Handbook of Conducting Polymers*, 3rd ed.; Skotheim, T. A., Reynolds, J. R., Eds.; CRC Press: Boca Raton, FL, 2007; Vol. *1*, pp 9-1−9-49.

(13) (a) Jeffries-El, M.; Sauvé, G.; McCullough, R. D. *Macromolecules* **2005**, *38*, 10346–10352. (b) Chen, T.-A.; Wu, X.; Rieke, R. D. *J. Am. Chem. Soc.* **1995**, *117*, 233–244.

(14) Since NMR signal integration can only be done with a certain degree of error, the percent regioregularities for **P1b** and **P1c** reported herein represent the lowest values for each polymer obtained from a few independent NMR experiments.

(15) Mao, Y.; Wang, Y.; Lucht, B. L. *J. Polym. Sci., Part A: Polym. Chem.* **2004**, *42*, 5538–5547.

(16) (a) Iovu, M. C.; Sheina, E. E.; Gil, R. R.; McCullough, R. D. *Macromolecules* **2005**, *38*, 8649–8656. (b) Miyakoshi, R.; Yokoyama, A.; Yokozawa, T. *J. Am. Chem. Soc.* **2005**, *127*, 17542–17547.

(17) Costanzo, P. J.; Stokes, K. K. *Macromolecules* **2002**, *35*, 6804–6810.

(18) (a) Coessens, V.; Pintauer, T.; Matyjaszewski, K. *Prog. Polym. Sci.* **2001**, *26*, 337–377. (b) Pyun, J.; Kowalewski, T.; Matyjaszewski, K. *Macromol. Rapid Commun.* **2003**, *24*, 1043–1059. (c) Balamurugan, S.; Mendez, S.; Balamurugan, S. S.; O'Brien, M. J., II; López, G. P. *Langmuir* **2003**, *19*, 2545–2549.

(19) McCullough, R. D.; Lowe, R. D. *J. Chem. Soc., Chem. Commun.* **1992**, 70–72.

(20) (a) Kiriy, N.; Jähne, E.; Adler, H.-J.; Schneider, M.; Kiriy, A.; Gorodyska, G.; Minko, S.; Jehnichen, D.; Simon, P.; Fokin, A. A.; Stamm, M. *Nano Lett.* **2003**, *3*, 707–712. (b) Langeveld-Voss, B. M. W.; Janssen, R. A. J.; Christiaans, M. P. T.; Meskers, S. C. J.; Dekkers, H. P. J. M.; Meijer, E. W. *J. Am. Chem. Soc.* **1996**, *118*, 4908–4909. (c) Zahn, S.; Swager, T. M. *Angew. Chem., Int. Ed.* **2002**, *41*, 4226–4229.

(21) (a) Brustolin, F.; Goldoni, F.; Meijer, E. W.; Sommerdijk, N. A. J. M. *Macromolecules* **2002**, *35*, 1054–1059. (b) Garreau, S.; Leclerc, M.; Errien, N.; Louarn, G. *Macromolecules* **2003**, *36*, 692–697. (c) Lévesque, I.; Leclerc, M. *Chem. Mater.* **1996**, *8*, 2843–2849. (d) Faïd, K.; Fréchette, M.; Ranger, M.; Mazarolle, L.; Lévesque, I.; Leclerc, M.; Chen, T.-A.; Rieke, R. D. *Chem. Mater.* **1995**, *7*, 1390–1396.

(22) Kim, J.; Swager, T. M. *Nature* **2001**, *411*, 1030–1034.

(23) Theander, M.; Inganäs, O.; Mammo, W.; Olinga, T.; Svensson, M.; Andersson, M. R. *J. Phys. Chem. B* **1999**, *103*, 7771–7780.

(24) Levitus, M.; Schmieder, K.; Ricks, H.; Shimizu, K. D.; Bunz, U. H. F.; Garcia-Garibay, M. A. *J. Am. Chem. Soc.* **2001**, *123*, 4259–4265.

(25) Pinto, M. R.; Kristal, B. M.; Schanze, K. S. *Langmuir* **2003**, *19*, 6523–6533.

(26) Dias, F. B.; Knaapila, M.; Monkman, A. P.; Burrows, H. D. *Macromolecules* **2006**, *39*, 1598–1606.

(27) (a) Zhulina, E. B.; Borisov, O. V.; Pryamitsyn, V. A.; Birshtein, T. M. *Macromolecules* **1991**, *24*, 140–149. (b) Baulin, V. A.; Zhulina, E. B.; Halperin, A. *J. Chem. Phys.* **2003**, *119*, 10977–10988. (c) Zhang, W.; Zhou, X.; Li, H.; Fang, Y.; Zhang, G. *Macromolecules* **2005**, *38*, 909–914.

(28) This gradual PNIPAm side chains "precollapse" at the temperatures below LCST apparently could not affect the backbone conformation of the regiorandom copolymer **P3a**, in which case no spectral changes were observed in this temperature range. This was probably due to the already significantly twisted backbone conformation of this copolymer, which made any further twisting more unfavorable and requiring really major changes of the side chains (like the phase transition at LCST).

(29) Hamley, I. W. *Introduction to Soft Matter: Synthetic and Biological Self-Assembling Materials*, revised ed.; Wiley: Chichester, UK, 2007.

(30) Reynolds, G. A.; Drexhage, K. H. *Opt. Commun.* **1975**, *13*, 222–225.

(31) Taranekar, P.; Qiao, Q.; Jiang, H.; Ghiviriga, I.; Schanze, K. S.; Reynolds, J. R. *J. Am. Chem. Soc.* **2007**, *129*, 8958–8959.